Solar RRL

WILEY VCH

Solar RRL

RESEARCH ARTICLE OPEN ACCESS

A Failure Mode Affecting the Reliability of LECO-Treated High-Efficiency TOPCon Solar Cells

Yuelin Xiong[1] | Tarek O. Abdul Fattah[1] | Kuninori Okamoto[2] | Ruy S. Bonilla[1]

[1]Department of Materials, University of Oxford, Oxford, UK | [2]Changzhou Fusion New Materials Co. Ltd, Shanghai, China

Correspondence: Ruy S. Bonilla (sebastian.bonilla@materials.ox.ac.uk)

Received: 28 February 2025 | **Revised:** 28 April 2025 | **Accepted:** 28 April 2025

Funding: Royal Academy of Engineering, Grant/Award Number: RF\201819\18\38; Engineering and Physical Sciences Research Council, Grant/Award Numbers: EP/V038605/1 EP/X037169/1; Leverhulme Trust, Grant/Award Number: RPG-2020-377

Keywords: contact resistance | LECO | metalization | reliability | TOPCon solar cells

ABSTRACT

Laser-enhanced contact optimization (LECO) has become an essential process in enabling the fabrication of >25% efficient tunnel oxide–passivated contact (TOPCon) solar cells, now in use in >100 GW of silicon solar module production. LECO improves the metal–semiconductor interface in silicon solar cells, thus resulting in an excellent trade-off between contact resistance ($\rho_c < 1$ mΩ.cm^2) and surface recombination ($J_{0met} < 160$ fA/cm^2). This work presents a new failure mode observed at the front p$^+$-Ag contact in LECO-treated TOPCon solar cells, which is not observed in standard screen-printed metallization. The bias and temperature stress severely degrade the dark contact resistance in LECO-treated TOPCon, leading to an increase in series resistance of over 100 Ω in a 2 x 2 cm^2 cell. Unlike standard TOPCon, where degradation has been ascribed to the n$^+$-Ag contact, the LECO cells show the most prominent degradation at the p-type contact side. Luminescence measurements on stressed samples show reduced recombination, which could be attributed to improved passivation at the p$^+$-Ag interface and/or the enhancement of other recombination-limiting factors such as AlO_x passivation, but negatively impacting conductivity. The temperature and bias stress also deteriorate the light current–voltage characteristics for the samples that underwent the LECO process. These results reveal a potential degradation mode in LECO-treated TOPCon solar cells, indicating the need for further investigation into its impact on efficiency gain, long-term reliability, and bankability.

1 | Introduction

Tunnel oxide–passivated contact (TOPCon) solar cells have emerged as a leading technology for achieving high-efficiency silicon solar cells. According to the International Technology Roadmap for Photovoltaics (ITRPV), TOPCon currently accounts for approximately 50% of the market share across all cell technologies, and it is expected to grow further in the coming years [1]. With a conversion efficiency exceeding 26.5%, excellent long-term reliability, and low-temperature sensitivity, this technology is well-positioned for widespread industrial adoption [2, 3]. Despite these advantages, a remaining significant challenge is establishing an effective Ohmic contact between the silver electrodes and the lowly doped boron emitters [4].

Advancements in laser-induced metalization technologies have shown that they can address this challenge by improving the contact quality on the front side of TOPCon cells. One such approach is the laser-enhanced contact optimization (LECO) process, which involves applying a high-intensity laser to the front side of the solar cell while maintaining a reverse voltage across the cell contacts [5]. This process induces a localized high current density at the contact interface, promoting interdiffusion between the silver and silicon materials, which reduces contact resistance and improves cell efficiency [6]. LECO is especially

effective in TOPCon cells, where it helps achieve low contact resistivity while maintaining good interface passivation at the p-side, thus enhancing open-circuit voltage (V_{oc}) and fill factor (FF) simultaneously [7]. This process has shown efficiency gains of up to $0.6\%_{abs}$ in experimental settings for TOPCon cells and was scaled up for mass production [6, 8]. Despite their forecast of widespread adoption, there is limited data regarding the reliability of LECO-treated TOPCon solar cells, indicating that failure mechanisms have not been revealed or understood.

Before the LECO step, high-temperature firing and hydrogenation steps of metal contacts are applied in the fabrication of industrial TOPCon solar cells [5]. These steps drive hydrogen from the dielectric layers, such as aluminum oxide and silicon nitride, into the surface and bulk of crystalline silicon to passivate defects and improve performance [9, 10]. However, under certain conditions, hydrogen-related interactions can also lead to an increase in R_s following thermal annealing. Hamer et al. demonstrated that applying a current during the thermal process can cause R_s to increase by an order of magnitude. They also highlighted that the direction of the applied electric field has a significant impact on the extent of this effect [11, 12]. Building on this, Liu et al. showed that the increase in R_s predominantly occurs at the interface between the Ag contact and the n-type side under forward bias, in both PERC and TOPCon solar cells [13]. This phenomenon highlights a broader reliability issue for solar cells in operation, as the increase in R_s can directly impact the device's long-term stability and efficiency.

In this study, we investigate a specific failure mode in LECO-treated TOPCon solar cells, which involves the degradation in series resistance of the cell after temperature and bias treatment. To probe this phenomenon, we applied independent bias cycles in a forward–reverse-forward–reverse order, systematically monitoring the changes in series resistance throughout the process. Electroluminescence (EL) and photoluminescence (PL) imaging techniques were employed to analyze the spatial distribution of series resistance and evaluate the passivation quality of the cells after exposure to thermal and electrical stress. And, 1 sun *I–V* measurements were carried out to understand the effect of the applied treatments on the device's electrical output. We show, for the first time, that hydrogen-induced contact resistance occurs at the Ag/p-type Si interface in LECO-treated TOPCon cells under specific temperature and bias conditions, highlighting the need for further studies to determine its relevance in long-term performance.

2 | Results and Discussion

We performed in situ *I–V* monitoring during 400°C annealing on both a standard TOPCon (s-TOPCon) cell and an LECO-treated TOPCon (LECO-TOPCon) cell to enable a comparative analysis. Figure 1 presents the changes in series resistance (ΔR_s) observed during the application of four bias cycles in the forward–reverse–forward–reverse order. Figure 1a illustrates the resistance changes in a reference s-TOPCon cell. A continuous increase in series resistance was observed during the first cycle of forward bias, while reverse bias resulted in a slight decrease in series resistance. Such degradation aligns with previously reported findings in the literature, which attributed the resistance increase to the passivation of the silver/n^+-polysilicon interface [13]. When analyzing the LECO-TOPCon cells (Figure 1b), the forward bias condition leads to a decrease in series resistance, which is the opposite of what was observed in s-TOPCon. Most staggeringly, the reverse bias in LECO-TOPCon severely degrades the series resistance, increasing it by over two orders of magnitude for the duration of 30 min. Useful indications can be drawn from data in Figure 1b: the process is cyclical, indicating that the polarity of the bias is important and that a charged species is involved in the resistance changes. As with most of the recent silicon cell instability mechanisms, the involvement of hydrogen is likely [11, 13, 14].

While both the Ag/p-Si and Ag/n-poly-Si contacts exhibit an increase in specific contact resistance from transfer length measurement (TLM) results, their individual contributions to the overall resistance increase shown in Figure 1 are not directly separated in our measurements. Since the LECO treatment is primarily designed to improve the front p-side contact in TOPCon cells, the front-side contact resistivity is a critical parameter for identifying the source of LECO-related reliability issues. The contact resistance measurement is performed after completing the full forward–reverse–forward–reverse bias cycles. Figure 2a,b shows TLM results used to extract contact resistivity

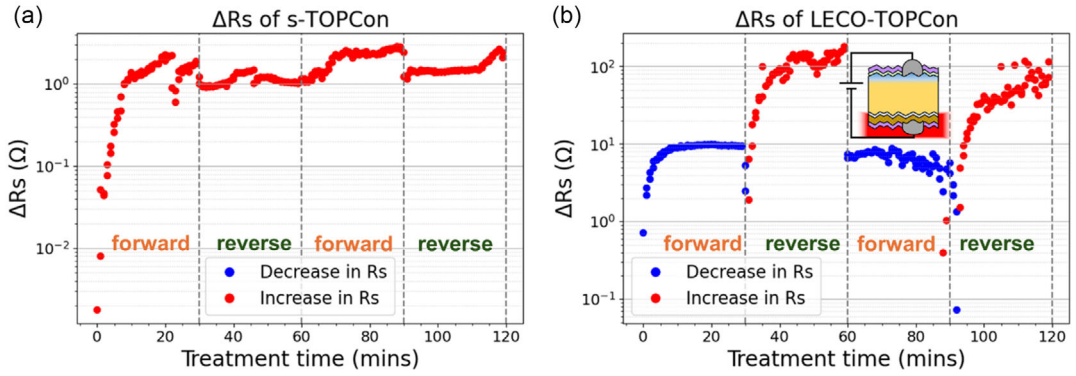

FIGURE 1 | The changes in series resistance relative to the starting value, ΔR_s as a function of annealing time for (a) TOPCon reference and (b) LECO-treated TOPCon solar cells. The samples were subjected to a cycle of 0.5 A forward current for 30 min followed by 0.5 V reverse bias for 30 min at 400°C. The blue markers indicate a decrease in R_s and the red markers indicate an increase in R_s.

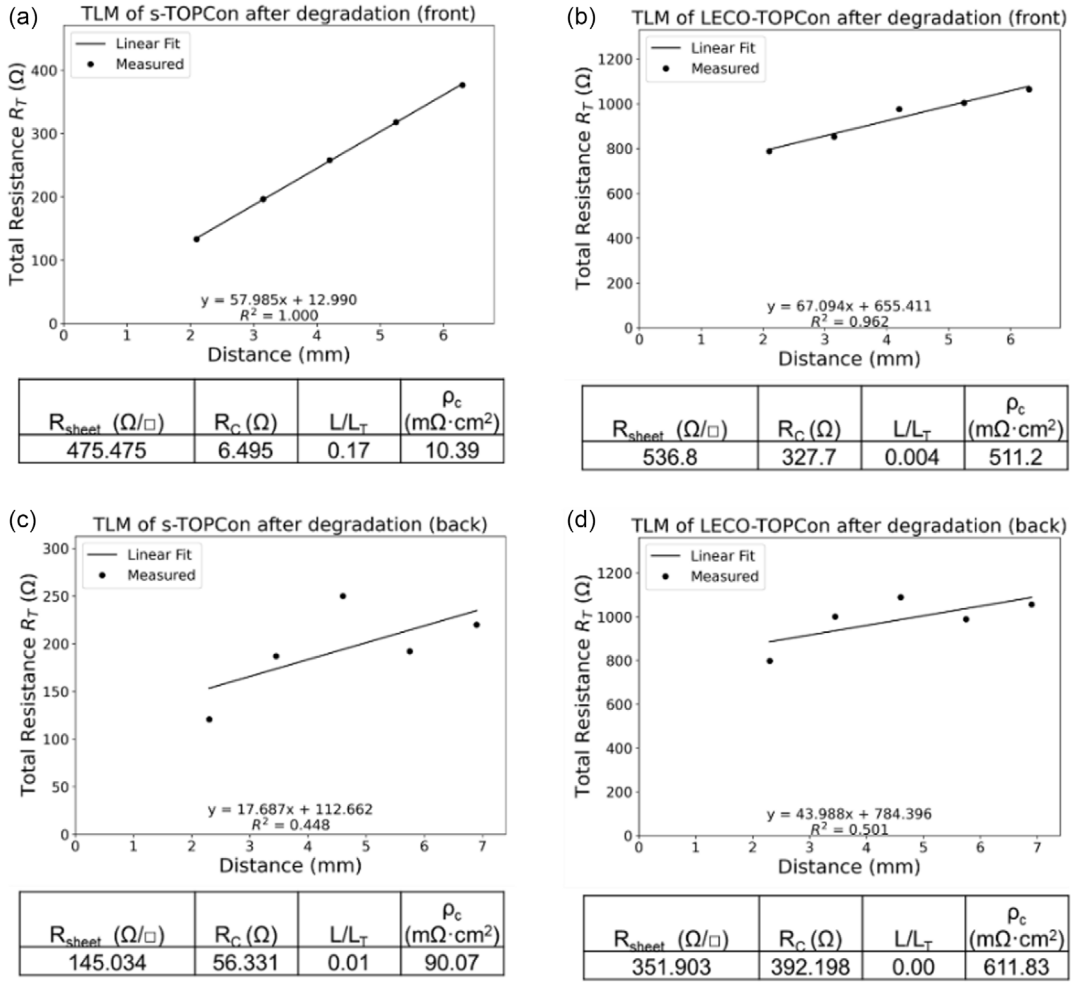

R_{sheet} (Ω/□)	R_C (Ω)	L/L_T	ρ_c (mΩ·cm²)
475.475	6.495	0.17	10.39

R_{sheet} (Ω/□)	R_C (Ω)	L/L_T	ρ_c (mΩ·cm²)
536.8	327.7	0.004	511.2

R_{sheet} (Ω/□)	R_C (Ω)	L/L_T	ρ_c (mΩ·cm²)
145.034	56.331	0.01	90.07

R_{sheet} (Ω/□)	R_C (Ω)	L/L_T	ρ_c (mΩ·cm²)
351.903	392.198	0.00	611.83

FIGURE 2 | TLM measurements of the front side for (a) s-TOPCon and (b) LECO-TOPCon solar cells after degradation, and of the back side for (c) s-TOPCon and (d) LECO-TOPCon solar cells after degradation. Extracted parameters are detailed in the following table.

on the front side for both the s-TOPCon and LECO-TOPCon cells after the degradation in Figure 1b. They reveal that the p-side contact in the LECO-TOPCon cell experienced significant degradation, with a contact resistance reaching over 320 Ω (Figure 2b), well above the original 4.8 Ω value. The TLM measurements before degradation are shown in Figure S1 (Supporting Information). In contrast, Figure 2a shows no such degradation in the p-side contact of the s-TOPCon cell.

Similar measurements of the back contact resistivity are presented in Figure 2c,d. It can be observed that both the s-TOPCon and LECO-TOPCon cells exhibited degradation in the rear contact following the temperature and bias treatment. The rear-side R_c increased from 0.5 to over 56 Ω in the s-TOPCon cell and from 0.7 to 392 Ω in the LECO-TOPCon cell. This degradation aligns with literature findings of degradation associated with the silver contact and the n-type interface [13].

As received and temperature/bias stressed specimens were characterized with EL/PL. Uniform EL emission in the as-received LECO-TOPCon specimens is shown in Figure 3a, indicating low and consistent contact resistance across the 4 cm^2 token. After stressing (Figure 3b), the increases in series resistance match an overall decrease in EL yield. High emission hot spots are evident, showing that only certain sections of the metalization pattern remain in good contact with the silicon underneath. The fingers are darkened significantly more than the bus bars, suggesting a more serious increase in series resistance in the p^+-Ag contact underneath the fingers. At this stage, no direct indication can be drawn to explain this observation and whether or not specific sections of the finger suffer more than others.

PL imaging results complement the resistance reliability findings shown earlier. In the as-received specimen, the PL yield is uniform (Figure 3c), with dark lines only appearing in the location of the contacts. This is expected as the metalization blocks light from reaching the PL camera sensor. Following bias stress and temperature treatments, an overall increase in the PL yield throughout the same cell is observed (Figure 3d), indicating a reduction in total recombination losses. These results could draw a link between the increased contact resistance and the presence of a passivating species, likely hydrogen, which mitigates recombination losses during the stressing procedure. A similar increase in PL yield was also observed in s-TOPCon following the same treatments shown in Figure S2 (Supporting Information). This means that the improvement in PL intensity could be due to either widespread improved passivation across the silicon surface (such as AlO_x passivation), or a potential passivation of the

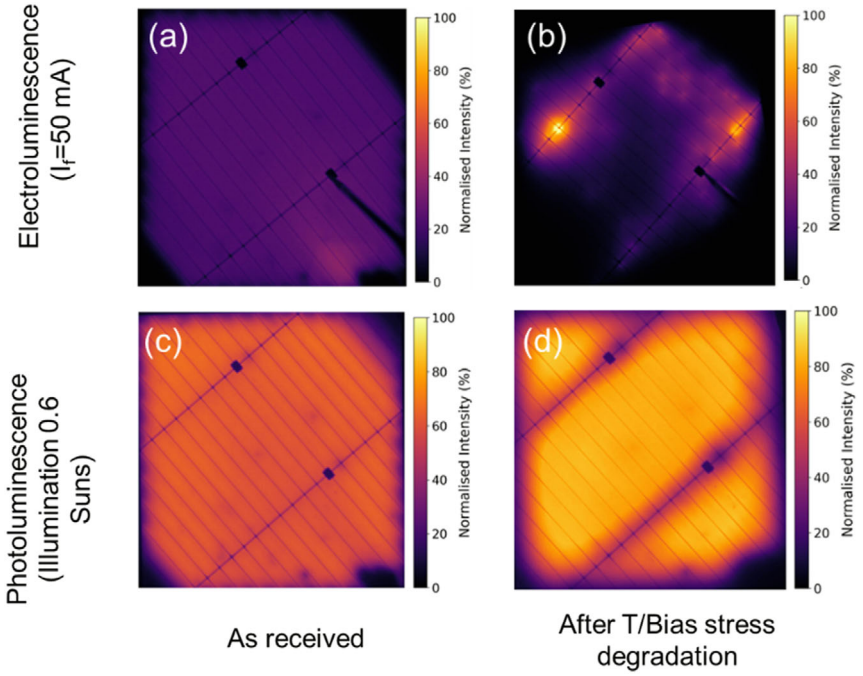

FIGURE 3 | Electroluminescence and photoluminescence images of (a), (c) as received and (b), (d) temperature-bias-treated LECO-treated TOPCon solar cell. Current and illumination settings used to take these images are shown. The scale bar represents the normalized percentage change in intensity.

metal/Si interface, which increases contact resistance and leads to a partial electrical isolation of the contacts from the rest of the device [15]. Another important observation is that the bus bars exhibit the highest recombination activity, while the regions beneath the fingers demonstrate improved passivation. This effect further supports the conclusion that the series resistance issue is primarily associated with the fingers rather than the bus bars. A plausible explanation for this is that bus bars use a different paste than the fingers, which prevents direct contact with the silicon before firing and results in only partial contact with the silicon after firing. This results in a distinct interface structure compared to that of the fingers. Overall, the EL and PL data indicate that the stressing conditions increase contact resistance but improve contact passivation conditions.

Following the observed increase in R_s under reverse bias, its impact on overall device performance was investigated. Figure 4 presents the light current density–voltage (J–V) curves (left) and the extracted solar cell parameters (right) for s-TOPCon and LECO-TOPCon, before and after 1 cycle (30 min) of reverse bias treatment at 400°C. Note that the efficiencies recorded show lower values than those in a full-area cell, due to losses from laser dicing and wire resistance in our I–V probe setup. The I–V results are only indicative of relative changes.

The s-TOPCon devices exhibited stable behavior, with no significant changes in performance after treatment. In contrast, the LECO-treated showed a drastic reduction in short-circuit current, J_{sc}, decreasing from 40.16 to 4.33 mA/cm^2, while preserving a nearly constant open-circuit voltage, V_{oc}. As a result, the FF and efficiency declined by ~50% and ~95% of their starting values, respectively. These results reveal that both temperature and reverse bias treatments not only lead to an increase in R_s, but also severely compromise the solar cell performance. The

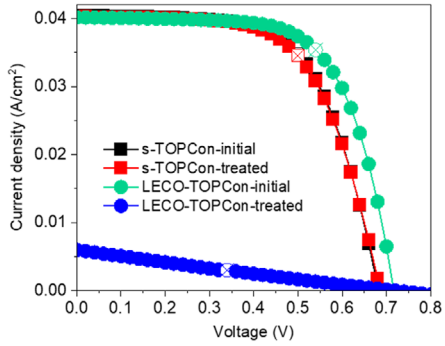

		V_{oc} [mV]	J_{sc} [mA/cm^2]	FF [%]	η [%]
s-TOPCon	Initial	681.8	40.38	63.2	17.41
	Treated	685.6	40.22	62.6	17.26
LECO-TOPCon	Initial	716.6	40.16	66.3	19.09
	Treated	719.1	4.33	32.6	1.02

FIGURE 4 | Light J–V curves of standard and LECO-treated TOPCon solar cells, with the maximum power point indicated by an empty cross symbol. The extracted solar cell parameters from light J–V measurements for both cells are shown in the table. The word "treated" refers to a reverse bias treatment of 0.5 V for 30 min at 400°C. Areas of s-TOPCon and LECO-TOPCon devices were 3.61 and 3.44 cm^2, respectively.

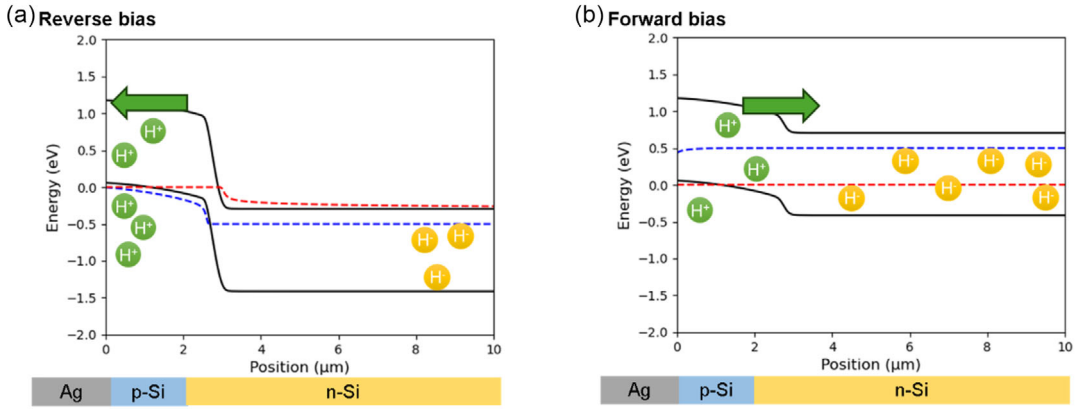

FIGURE 5 | A possible physical model for hydrogen-induced contact resistance in LECO-treated TOPCon devices under (a) reverse bias and (b) forward bias. Band diagrams obtained by a solar cell capacitance simulator (SCAPS) finite element device simulation.

observed reduction in efficiency cannot be attributed solely to the increase in R_s, suggesting the involvement of additional mechanisms that will require a separate investigation.

The significant impact that the reverse bias annealing has on both R_s and the performance of LECO-TOPCon cells urges a deeper microscopic understanding of the occurrence of degradation. We attempt to establish a preliminary model for the failure mechanism involved in the increased R_s based on hydrogen, as shown in Figure 5. The model considers how the polarity of the electric field dictates the direction of hydrogen species transport, influencing interface passivation and charge carrier dynamics [16].

Under reverse bias (Figure 5a), the increased potential barrier directs positively charged hydrogen H^+ in the B-doped emitter to the p^+-Ag front interface, where they accumulate and passivate interface states. This passivation alters the band alignment at the interface, leading to an increase in the Schottky barrier height [13, 17]. The redistribution of charge also induces a space charge region, changing the charge carrier concentration and further increasing the energy barrier for the flow of holes into the Ag contact. Therefore, it contributes to the observed increase in R_s for LECO-treated contacts.

Since LECO improves contact properties, it modifies the defect landscape at the Ag/Si interface. As a result, hydrogen accumulation is more pronounced at the LECO-treated contact/Si interface because fewer unpassivated defects remain to be passivated by hydrogen. Therefore, the excess hydrogen leads to a more significant increase in R_s for LECO-TOPCon compared to s-TOPCon. The PL imaging results also support this hypothesis.

Conversely, under forward bias in Figure 5b, hydrogen migrates from the p-type to the n-type region, transitioning from H^+ to H^-. As a result, the concentration of H^+ at the p^+-Ag front interface is reduced, facilitating carrier transport and avoiding the increase in R_s. The full picture behind the deterioration in the performance of LECO-TOPCon solar cells remains unclear at this stage, with this proposed model being highly hypothetical. The relationship between the movement of hydrogen and the observed degradation in J_{sc} and FF will be assessed and established in future work.

Given that solar cells operate under forward bias in the field, improvements in R_s are expected based on our findings in Figure 1. However, the efficiency deterioration triggered by the reverse bias and temperature stress opens the question to whether this effect is related to the combination of these conditions or can also occur under thermal stress only. If temperature is the main component causing the issue, this could still be detrimental for solar cells operating in the field. Further investigations will be required to decouple these components and better examine the impact of bias/temperature on solar cell performance.

3 | Conclusions

A new failure mode in LECO-treated TOPCon solar cells has been revealed. Our study demonstrates that reverse bias stress at high temperatures significantly degrades the p^+-Ag contact, increasing series resistance and degrading the solar cell performance thus compromising cell reliability. In contrast, samples not exposed to the LECO process showed a decrease in R_s upon forward bias treatment and stable R_s and J–V characteristics upon reverse bias treatments. This reliability issue was confirmed through in situ dark I–V and transfer line measurements. Monitoring the changes in luminescence yield from LECO-treated samples exposed to temperature-bias stress shows improved passivation. While the LECO process typically reduces contact resistance and enhances efficiency, our findings point toward improved passivation properties but hindered conductivity under stress, which could be related to p^+-Ag and/or AlO_x interfaces. The significant impact of electric field direction suggests the potential involvement of hydrogen in resistance changes. Based on these observations, a preliminary model is proposed to explain the observed change in resistance.

If not addressed, this degradation could influence the long-term performance and economic viability of LECO-treated cells, raising questions about their ability to meet industry durability standards. A reduction in cell lifespan and efficiency could impact energy yield and financial returns, especially at a time when solar energy is crucially needed. Further investigations are required to understand the microscopic nature of this

reliability issue and explore potential mitigation strategies for enhancing stability under operational conditions.

4 | Experimental Section

4.1 | Sample Preparation

The preparation of TOPCon cells follows the standard industrial process, wherein silver pastes were screen-printed onto silicon wafers and subjected to rapid firing to form the front and back silver electrodes. Following this, the cells underwent LECO treatment, which involved applying a reverse bias voltage to both sides of the cells while performing a laser scan perpendicular to the front Ag electrodes. In this work, TOPCon solar cells were sourced from an industrial partner, bearing either standard higher-temperature fired screen-printed silver contacts or LECO-treated contacts with lower firing temperatures. Both s-TOPCon and LECO-TOPCon cells were fabricated on an n-type silicon base with a resistivity of ~1–2 Ω·cm. The front side features a boron-diffused emitter with a resistivity of 420 Ω/□, passivated by an AlO_x/SiN_x stack. On the rear side, a tunneling SiO_x layer was deposited, followed by a 90–110 nm n-type polysilicon layer. The rear passivation stack consists of AlO_x and SiN_x. Front metalization was achieved using an Ag/Al contact, whereas the LECO-TOPCon paste does not rely on aluminum for contact. The paste for the bus bars is non-fire-through. The s-TOPCon cells showed an average efficiency of 22.5%, while the LECO-TOPCon cells recorded a 25.2% average performance across 8 M12 cells. It should be noted that the s-TOPCon cells were fabricated using a process optimized for LECO, including a low emitter doping, and therefore represent a non-standard process when LECO is not present. The samples used in this study were prepared from commercial M12 TOPCon silicon cells, which were then cleaved into ~$2 \times 2\,cm^2$ tokens. Our findings here reflect the combined effects of the LECO process, which involves both a lower firing temperature and the LECO treatment.

4.2 | Measurement Setup

We performed in situ *I–V* monitoring on both s-TOPCon cell and LECO-TOPCon cell to enable a comparative analysis. The series resistance test for LECO-TOPCon was carried out on five samples, with each of them showing a similar behavior under forward and reverse bias. The samples were taken from 2 M12 solar cells, both of which exhibited standard solar cell properties prior to cutting.

All specimens were tested in a dark box. A closed-loop-controlled hot plate was used to heat the sample to 400°C, with a mechanically affixed thermocouple and a proportional-integral-derivative controller ensuring precise temperature regulation. A Keithley 2401 source measuring unit was used for in situ monitoring of *I–V* characteristics and the application of bias stress. Figure 6 illustrates the geometry of the TOPCon solar cell provided by an industrial manufacturer and the temperature-dependent *I–V* measurement setup. Forward (0.5 A) and reverse bias (0.5 V) cycles were applied to the samples, with the cell series resistance (R_s) determined by measuring the *I–V* curve in the range of −0.2 to 0.2 V in the dark at elevated temperatures. R_s includes the resistance from the front contact to the rear contact, as well as the internal resistance within the device. The change in series resistance (ΔR_s) was calculated using the initial R_{s0} as the baseline value. ΔR_s was plotted on a logarithmic scale to account for the different magnitudes of change observed under forward and reverse bias conditions.

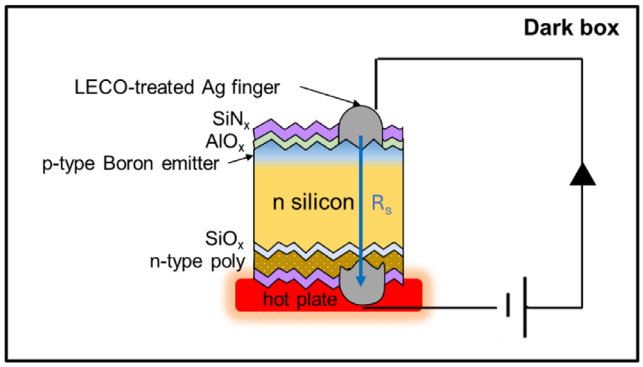

FIGURE 6 | Schematic of the measurement setup for in situ measurement of R_s under temperature and bias stress.

After the stressing routine, the samples were diced into strips without a bus bar to enable TLMs of contact resistance. The total resistance was measured as a function of the distance between the fingers. The finger pitch was measured using an optical microscope, with the front finger pitch determined to be 1.05 mm and the back finger pitch measured at 1.15 mm. The contact resistance was extracted from the intercept of the total resistance versus distance plot as detailed in ref. [18].

PL and EL imaging were conducted using a BrightSpot Automation setup. PL imaging was used to visualize carrier density under stable illumination at 0.6 suns, enabling the characterization of spatial recombination across the cell. EL imaging was employed to map the series resistance distribution by applying a forward bias current ($I_f = 50$ mA) using a GW Instek GSM-20H10 source measure unit, providing a comparative analysis of the cell's performance before and after the temperature and bias degradation process.

Dark *J–V* curves were measured using a Keithley 2401 source measure unit in a four-wire configuration within a dark box. Light *J–V* measurements were performed using a LOT-QuantumDesign Europe LS0505 sun simulator, with a GW Instek GSM-20H10 source measure unit. Standard testing conditions included an air mass 1.5G spectrum with an intensity of 100 mW/cm^2, calibrated using a standard silicon reference cell. Uniform illumination was provided over a 40×40 mm area at a controlled temperature of 25°C, maintained by a thermal system.

Acknowledgements

All the authors are thankful to Juan Camilo Gutiérrez for assistance in building the setup and James McQueen for the SCAPS TOPCon model. R.S.B was supported by the Royal Academy of Engineering under the Research Fellowship scheme (grant no. RF\201819\18\38). This work was supported by the Leverhulme Trust Prize, Research Project Grant

(RPG-2020-377), the UK Engineering and Physical Sciences Research Council grant numbers EP/V038605/1 and EP/X037169/1, and by the Oxford University John Fell Fund. For the purpose of Open Access, the author has applied a CC BY public copyright license to any Author Accepted Manuscript (AAM) version arising from this submission.

Conflicts of Interest

The authors declare no conflicts of interest.

Data Availability Statement

All data created during this research and published in this article is openly available from the Oxford University Research Archive and can be downloaded free of charge from http://ora.ox.ac.uk.

References

1. International Technology Roadmap for Photovoltaic (ITRPV), 2024, accessed May 20, 2024, https://www.vdma.org/international-technology-roadmap-photovoltaic.

2. Trina Solar, "*AP/Trinasolar Announces Efficiency of* 26.58% for *n-Type TOPCon Cells, Setting the 28th World Record*," accessed January 24, 2025, https://static.trinasolar.com/en-apac/resources/newsroom/aptrinasolar-announces-efficiency-2658-n-type-topcon-cells-setting-28th-world.

3. J. Zhou, X. Su, Q. Huang, et al., "Recent Advancements in Poly-Si/SiOx Passivating Contacts for High-Efficiency Silicon Solar Cells: Technology Review and Perspectives," *Journal of Materials Chemistry A* 10, no. 38 (2022): 20147–20173, https://doi.org/10.1039/D2TA04730F.

4. Y. Li, R. Zhou, Z. Chen, et al., "Insight into the Contact Mechanism of Ag/Al-Si Interface for the Front-Side Metallization of TOPCon Silicon Solar Cells," *Small Methods* 9, no. 1 (2025): 2400707, https://doi.org/10.1002/smtd.202400707.

5. S. Groser, E. Krassowski, S. Swatek, H. Zhao, and C. Hagendorf, "Microscale Contact Formation by Laser Enhanced Contact Optimization," *IEEE Journal of Photovoltaics* 12, no. 1 (2022): 26–30, https://doi.org/10.1109/JPHOTOV.2021.3129362.

6. T. Fellmeth, H. Höffler, S. Mack, et al., "Laser-Enhanced Contact Optimization on, *i*, TOPCon Solar Cells," *Progress in Photovoltaics* 30, no. 12 (2022): 1393–1399, https://doi.org/10.1002/pip.3598.

7. E. Krassowski, D. Hevisov, S. Großer, and M. Turek, "*Investigation of Impact of Cell-Properties on LECO Effectiveness Using Off-Spec PERC-Cells of Different Manufacturers on MK4 Platform*," in Proceedings of the 10th Workshop on Metallization and Interconnection for Crystalline Silicon Solar Cells (Genk, Belgium, 2022), 020009, https://doi.org/10.1063/5.0126349.

8. A. Mette, S. Hörnlein, F. Stenzel, et al., "Q.ANTUM NEO with LECO Exceeding 25.5% Cell Efficiency," *Solar Energy Materials and Solar Cells* 277 (2024): 113110, https://doi.org/10.1016/j.solmat.2024.113110.

9. J.-I. Polzin, B. Hammann, T. Niewelt, W. Kwapil, M. Hermle, and F. Feldmann, "Thermal Activation of Hydrogen for Defect Passivation in Poly-Si Based Passivating Contacts," *Solar Energy Materials and Solar Cells* 230 (2021): 111267, https://doi.org/10.1016/j.solmat.2021.111267.

10. Y. Yang, P. P. Altermatt, Y. Cui, et al., "Effect of Carrier-Induced Hydrogenation on the Passivation of the Poly-Si/SiOx/c-Si Interface," *AIP Conference Proceedings* 1999 (2018): 040026, https://doi.org/10.1063/1.5049289.

11. P. Hamer, C. Chan, R. S. Bonilla, et al., "Hydrogen Induced Contact Resistance in PERC Solar Cells," *Solar Energy Materials and Solar Cells* 184 (2018): 91–97, https://doi.org/10.1016/j.solmat.2018.04.036.

12. C. Chan, P. Hamer, G. Bourret-Sicotte, et al., "Instability of Increased Contact Resistance in Silicon Solar Cells Following Post-Firing Thermal Processes," *Solar RRL* 1, no. 11 (2017): 1700129, https://doi.org/10.1002/solr.201700129.

13. D. Liu, M. Wright, M. Goodarzi, P. R. Wilshaw, P. Hamer, and R. S. Bonilla, "Observations of Contact Resistance in TOPCon and PERC Solar Cells," *Solar Energy Materials and Solar Cells* 246 (2022): 111934, https://doi.org/10.1016/j.solmat.2022.111934.

14. D. Chen, P. Hamer, M. Kim, et al., "Hydrogen-Induced Degradation: Explaining the Mechanism behind Light- and Elevated Temperature-Induced Degradation in n- and *p-Type* Silicon," *Solar Energy Materials and Solar Cells* 207 (2020): 110353, https://doi.org/10.1016/j.solmat.2019.110353.

15. M. Pawlik, J. P. Vilcot, M. Halbwax, et al., "Electrical and Chemical Studies on Al2O3 Passivation Activation Process," *Energy Procedia* 60 (2014): 85–89, https://doi.org/10.1016/j.egypro.2014.12.347.

16. B. J. Hallam, P. G. Hamer, A. M. Ciesla née Wenham, C. E. Chan, B. Vicari Stefani, and S. Wenham, "Development of Advanced Hydrogenation Processes for Silicon Solar Cells via an Improved Understanding of the Behaviour of Hydrogen in Silicon," *Progress in Photovoltaics: Research and Applications* 28, no. 12 (2020): 1217–1238, https://doi.org/10.1002/pip.3240.

17. S. Kim, S. M. Iftiquar, D. Lee, et al., "Improvement in Front-Contact Resistance and Interface Passivation of Heterojunction Amorphous/Crystalline Silicon Solar Cell by Hydrogen-Diluted Stacked Emitter," *IEEE Journal of Photovoltaics* 6, no. 4 (2016): 837–845, https://doi.org/10.1109/JPHOTOV.2016.2553779.

18. S. Guo, G. Gregory, A. M. Gabor, W. V. Schoenfeld, and K. O. Davis, "Detailed Investigation of TLM Contact Resistance Measurements on Crystalline Silicon Solar Cells," *Solar Energy* 151 (2017): 163–172, https://doi.org/10.1016/j.solener.2017.05.015.

Supporting Information

Additional supporting information can be found online in the Supporting Information section.